

Fig. 3 Transmittances of metallic films compared to ITO in visible wavelength

Thicknesses: 135 Å (Al), 27 Å (Ag), 120 Å (Au)

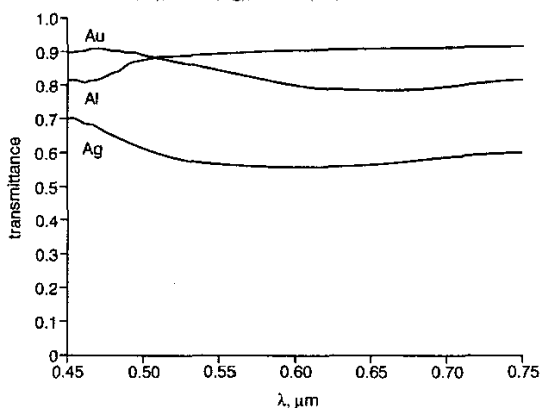


Fig. 4 High transmittance of very thin films of Au, Ag and Al

Thicknesses: Au and Al film, below 50 Å; Ag, below 15 Å

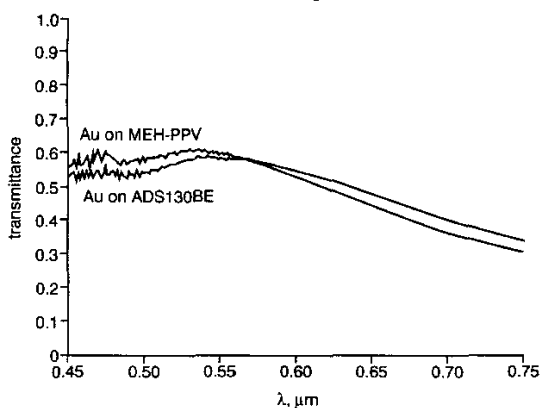


Fig. 5 Transmittance of Au on top of polymers

Conclusion: This work has found that Au films have better transmittance than Ag and Al. The 120 Å Au films have $\approx 60\%$ transmittance compared to 70% for ITO. Au films with transmittances reaching 80% were also obtained with a corresponding degradation in resistance. The most important aspect to note is that Au films may have promise as transparent contacts. The resistance and transmittance did not change significantly while they were tested in contact with two popular light-emitting polymers.

© IEE 2002

25 March 2002

Electronics Letters Online No: 20020527

DOI: 10.1049/el:20020527

Y. Guan and M.A. Matin (Department of Engineering, University of Denver, 2390 S. York St., Denver, CO 80208, USA)

E-mail: yguan@du.edu

T.M. Stephen (Department of Physics and Astronomy, University of Denver, 2390 S. York St., Denver, CO 80208, USA)

References

- BURROUGHS, J.H., BRADLEY, D.D.C., BROWN, A.R., MARKS, R.N., MACKAY, K., FRIEND, R.H., BURNS, P.L., and HOLMES, A.B.: 'Light-emitting diodes based on conjugated polymers', *Nature*, 1990, **347**, pp. 539–541
- SCOTT, J.C., KAUFMAN, J.H., BROCK, P.J., DIPIETRO, R., SALEM, J., and GOITIA, J.A.: 'Degradation and failure of MEH-PPV light-emitting diodes', *J. Appl. Phys.*, 1996, **79**, pp. 2745–2751
- SCHLATMANN, A.R., WILMS FLOET, D., HILBERER, A., GARTEN, F., SMULDERS, P.J.M., KLAPWIJK, T.M., and HADZIOANNOU, G.: 'Indium contamination from the indium-tin-oxide electrode in polymer light-emitting diodes', *Appl. Phys. Lett.*, 1996, **69**, pp. 1764–1766
- CAO, Y., TREACY, G.M., SMITH, P., and HEEGER, A.J.: 'Solution-cast films of polyaniline: optical-quality transparent electrodes', *Appl. Phys. Lett.*, 1992, **60**, pp. 2711–2713

Travelling wave distributed photodetectors with backward wave cancellation for improved AC efficiency

S. Murthy, T. Jung, M.C. Wu, D.L. Sivco and A.Y. Cho

In travelling wave distributed photodetectors, half the photocurrent generated in each individual photodiode is lost in the input termination. Here, a multi-section transmission line for cancellation of the backward travelling wave to achieve up to 6 dB improvement in the RF magnitude response without any bandwidth reduction is proposed and demonstrated.

Introduction: High-power, high-speed photodetectors reduce RF insertion loss, increase spurious free dynamic range and signal-to-noise ratio of analogue fibre optic links [1]. Velocity matched distributed photodetectors (VMDP), in which the periodic capacitance of the distributed diodes is used to match the microwave and optical velocities, have demonstrated high bandwidth and high saturation current by increasing the total absorption volume while summing up the electrical signal from the individual photodiodes in phase [2, 3]. As in the case of travelling wave photodetectors, the input end needs to be terminated with the line impedance (usually 50 Ω), otherwise, the phase lag between the currents travelling directly to the load and the reflection of currents travelling towards the input will decrease the bandwidth. The bandwidth improvement with input termination is, however, at the expense of efficiency as half of the current generated by the individual photodiodes is thrown away in the input 50 Ω termination. The RF response can be improved by cancelling out the backward propagating wave using a multi-section transmission line, as originally proposed for distributed amplification in travelling wave tubes [4]. A similar scheme for improving the efficiency of travelling wave distributed photodetectors has been proposed by [5, 6]. In this Letter, we propose and demonstrate a multi-section transmission line travelling wave distributed photodetector (MS-TWDP) with dissimilar coplanar strips (CPS) for backward wave cancellation. The line impedances of the different sections are designed to cancel out the backward propagating wave and thus improve RF response without degrading bandwidth. To our knowledge, this is the first experimental demonstration of backward wave cancellation in distributed photodetectors.

Theory: The backward wave propagating wave in any travelling wave scheme can be cancelled through a multi-section transmission line. The line impedances of the different sections are chosen such that the reflected portion of the forward propagating current is cancelled out by the fractional current which flows in the reverse direction due to current division (by Ohm's law). In the original publication [4], it was assumed that the current generated by each of the sources is the same. This leads to the following relation for the line impedance of the n th

section Z_n :

$$Z_n = \frac{Z_1}{n} \quad (1)$$

where Z_1 is the impedance of the first section. Equal distribution of photocurrents among the different diodes can be achieved using a monolithically integrated multimode interference (MMI) coupler for parallel optical feed [7]. For the case where the current sources are not equal, the following expression can be derived:

$$\frac{Z_n}{Z_{n+1}} = 1 + \frac{I_{n+1}}{I_n} \quad (2)$$

Backward wave cancellation transmission lines can thus be designed for any arbitrary current distribution among the photodiodes. This can be used to decrease the line impedance values to a realisable value.

Design and fabrication: The schematic diagram of the MS-TWDP is shown in Fig. 1. The devices were fabricated in the InAlGaAs system. The absorbing region is a 0.25 μm -thick layer of InGaAs with illumination from the p -side. We fabricated both the MS-TWDP and the single section travelling wave photodetector (SS-TWDP), to compare the performance. Each design consists of five diodes, which are 4 μm wide and are separated by 400 μm . The total absorption length is 85 μm in both cases, to ensure comparable responsivities. For the MS-TWDP, we chose a current distribution such that the first diode generates twice the photocurrent of each of the other diodes. The required impedance values for this current distribution can be calculated from (2) to be 150, 100, 75, 60 and 50 Ω from the input end to the load end. The highest line impedance is thus reduced from 250 Ω (for equal current distribution) to 150 Ω , which is easier to fabricate. The line impedance of the SS-TWDP was designed to be 50 Ω . The diode lengths and the CPS widths for the two designs are summarised in Table 1.

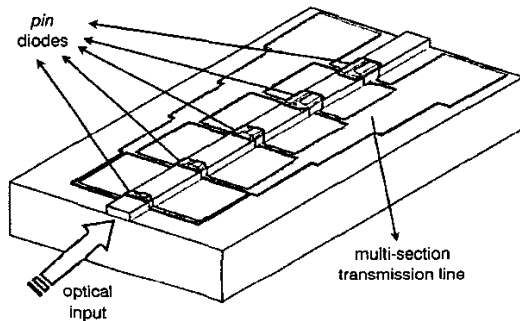


Fig. 1 Schematic diagram of multi-section travelling wave photodetector

Table 1: CPS and diode dimensions of fabricated MS-TWDP and SS-TWDP

Diode number	Diode length (μm)	CPS width (μm)	CPS separation (μm)
MS-diode 1	20	4	150
MS-diode 2	12	31	120
MS-diode 3	14	70	90
MS-diode 4	17.5	85	55
MS-diode 5	21.5	107	40
Each SS diode	17	120	30

The device mesas were patterned using conventional wet etching techniques and the metal patterns were defined using e-beam evaporation followed by liftoff. The p -contact is made by AuBe/Ti/Au deposition and the n -contact metal consists of Au/Sn/Au layers.

Results: The DC responsivity of the MS-TWDP is 0.23 A/W and that of the SS-TWDP is 0.25 A/W. The responsivity is limited by the fibre coupling loss and the Fresnel reflection loss at the waveguide interface. For microwave measurements, the photodetectors were mounted on an InP carrier substrate and the microwave signal collected using a

40 GHz GGB Industries probe. Chip resistors were wire bonded to the input end for measurements which required input termination. The impedance of the chip resistors were measured using a HP8510C network analyser. The resistance values vary by less than 10% in the measured frequency range (45 MHz–5 GHz). For the frequency response measurements, the photodetectors were illuminated with 9 dBm of 1.55 μm output from a Photonics external cavity diode laser. The RF signal is generated and detected in a Lightwave test set (HP83240A and HP8510C). The various frequency response measurements at a DC bias voltage of 3 V are shown in Fig. 2. In the case of the SS-TWDP, comparison of the response with the open input end to the response when the input end is terminated with 50 Ω shows the expected improvement in bandwidth at the expense of signal responsivity. The open input response is higher than the terminated response by a maximum of 6 dB at low frequencies. This is because half the current is absorbed in the input termination, which corresponds to a power difference of 6 dB. The bandwidth of the open SS-TWDP is however lower, as mentioned earlier. In the case of MS-TWDP, the response with the input end terminated decreases by only 1 to 2 dB compared to the open input response in the frequency range of measurement. Since the response reduction on input termination is a measure of the fraction of power travelling in the backward (towards input) direction, the plots in Fig. 2 show that less than 1 dB of current is flowing towards the input end. More importantly, the bandwidth of the MS-TWDP is comparable to those of the SS-TWDP with matched input termination. The AC response has thus been increased by a maximum of 6 dB without bandwidth reduction.

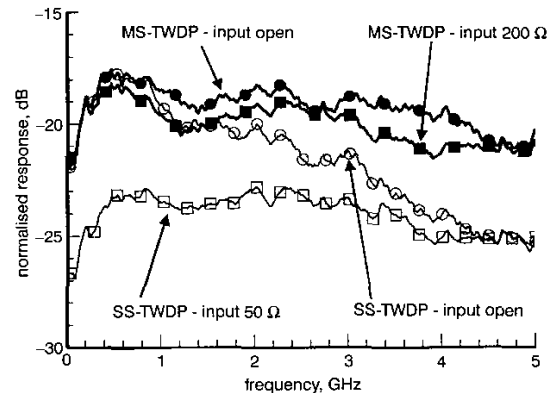


Fig. 2 Measured frequency response of SS-TWDP and MS-TWDP for open and terminated inputs

MS-TWDP shows up to 6 dB improvement of RF response without bandwidth degradation

Conclusion: RF responsivity of travelling wave photodetectors is increased by cancelling the backward propagating wave with a multi-section transmission line. We have experimentally shown that the RF response increases by 6 dB, without bandwidth reduction, in our multi-section travelling photodetector.

Acknowledgments: This work was supported by the Defense Advanced Research Program Agency (DARPA) under Contract N66011-98-1-8925.

© IEE 2002

5 March 2002

Electronics Letters Online No: 20020532

DOI: 10.1049/el:20020532

S. Murthy, T. Jung and M.C. Wu (Electrical Engineering Department, University of California, Los Angeles, CA 90095, USA)

E-mail: sanjeev@icsl.ucla.edu

D.L. Sivco and A.Y. Cho (Lucent Technologies, Bell Laboratories, Murray Hill, NJ 07974, USA)

References

- COX, C.H.: 'Gain and noise figure in analogue fiber-optic links', *IEE Proc. J, Optoelectron.*, 1992, **139**, (4), pp. 238–242

- 2 LIN, L.Y., WU, M.C., ITOH, T., VANG, T.A., MULLER, R.E., SIVCO, D.L., and CHO, A.Y.: 'High-power high-speed photodetectors - design, analysis, and experimental demonstration', *IEEE Trans. Microw. Theory Tech.*, 1997, 45, (8), pp. 1320-1331
- 3 ISLAM, M.S., MURTHY, S., ITOH, T., WU, M.C., NOVAK, D., WATERHOUSE, R.B., SIVCO, D.L., and CHO, A.Y.: 'Velocity-matched distributed photodetectors and balanced photodetectors with p-i-n photodiodes', *IEEE Trans. Microw. Theory Tech.*, 2001, 49, (10), pp. 1914-1920
- 4 GINZTON, E.L., HEWLETT, W.R., JASBERG, J.H., and NOE, J.D.: 'Distributed amplification', *Proc. IRE*, 1948, 36, pp. 956-969
- 5 NESNIDAL, M.P., DAVIDSON, A.C., EMMEL, G.R., MARSLAND, R.A., and WU, M.C.: 'Efficient, reliable, high-power VMDPs for linear fiber optic signal transmission'. Proc. of PSAA-10, Monterey, CA, USA, February 2000
- 6 SHI, J.-W., SUN, C.-K., and BOWERS, J.E.: 'Taper line distributed photodetector'. Tech. Dig., LEOS 2001, San Diego, CA, USA, November 2001, pp. 382-383
- 7 MURTHY, S., JUNG, T., CHAU, T., WU, M.C., SIVCO, D., and CHO, A.Y.: 'A novel monolithic distributed traveling-wave photodetector with parallel optical feed', *IEEE Photonics Technol. Lett.*, 2000, 12, (6), pp. 681-683

GaN MOSFET with liquid phase deposited oxide gate

Kuan-Wei Lee, Dei-Wei Chou, Hou-Run Wu, Jian-Jun Huang, Yeong-Her Wang, Mau-Phon Houng, Sou-Jinn Chang and Yan-Kuin Su

Liquid phase deposited SiO_2 as the insulating gate on an n -channel depletion mode GaN MOSFET is demonstrated. For a device with a $13\ \mu\text{m}$ source-to-drain distance and gate metal of $8 \times 40\ \mu\text{m}^2$, a transconductance of $48\ \text{mS/mm}$ and a drain current of $250\ \text{mA/mm}$ at $V_{gs} = 4\ \text{V}$ and $V_{ds} = 20\ \text{V}$ can be achieved.

Introduction: GaN MESFETs have been shown to be suitable for high-power and high-temperature microwave applications [1, 2]. The Schottky barrier may suffer gate swing voltage and gate leakage current, which may limit the device applications. The benefits of a MOSFET compared to its counterpart using a Schottky gate are lower gate current and higher gate swing voltage. Attempts have been made in pursuit of high-quality and low-interface defect density oxide layers on a GaN surface. However, the lack of reliable oxide (insulator) layers on GaN, and fewer reported on a GaN MOSFET, can be seen. Recently, the molecular beam deposited $\text{Ga}_2\text{O}_3(\text{Gd}_2\text{O}_3)$ on a GaN MOSFET as the gate insulator resulted in the first nitride MOSFET [3, 4]. In addition, CVD- SiO_2 [5, 6] and photoanodic oxide have been developed [7]. In this Letter, an alternative approach, the liquid phase deposition (LPD) method [8], is proposed for the formation of SiO_2 as the gate dielectrics for GaN MOSFET applications. It is simple, efficient and low cost to grow a uniform oxide layer on GaN operated near room temperature.

Experiment: The experimental setup consists of a temperature controller, pH meter and substrate holder. Supersaturated hydrofluosilicic acid aqueous solution (H_2SiF_6) as a source liquid and boric acid aqueous solution (H_3BO_3) as a deposition rate controller are used. GaN wafers were immersed into the $0.4\ \text{M}\ \text{H}_2\text{SiF}_6$ and $0.01\ \text{M}\ \text{H}_3\text{BO}_3$ solution at a pH value of -0.09 to form the desired oxide layer at 40°C . The deposition rate is $50\ \text{nm/h}$. Details of the LPD process on III-V compounds are given elsewhere [8, 9]. However, depositing silicon dioxide on GaN-based materials has, to the authors' knowledge, taken place for the first time. Selective oxide deposition can be also seen, i.e. smooth SiO_2 can be grown only on a GaN surface instead of metal or photoresistor. This provides potential for device applications.

The LPD oxide layer is applied to the gate dielectric of the n -channel GaN MOSFET on the MOCVD-grown structure as shown in Fig. 1. An undoped GaN buffer layer ($1\ \mu\text{m}$) was first grown on a (0001) c -plane sapphire substrate, followed by a $200\ \text{nm}$ -thick Si-doped ($\text{Nd} = 5 \times 10^{17}\ \text{cm}^{-3}$) GaN layer as the channel layer and, finally, a $20\ \text{nm}$ -thick capping layer with an Si-doped concentration of $\text{Nd} = 2 \times 10^{18}\ \text{cm}^{-3}$. Device mesa isolation was first formed by the photo-enhanced chemical etching method using KOH with $\text{pH} = 13.5$

and light intensity of $25\ \text{mW/cm}^2$. The etching rate is $50\ \text{nm/min}$. After forming the drain and source metals with Ti/Al/Au ($25/100/100\ \text{nm}$) with rapid thermal annealing at 900°C , LPD is performed to selectively deposit gate oxide and then define the Al gate pattern. In addition, the oxide as shown in the Figure will also automatically passivate the etched isolated surface wall.

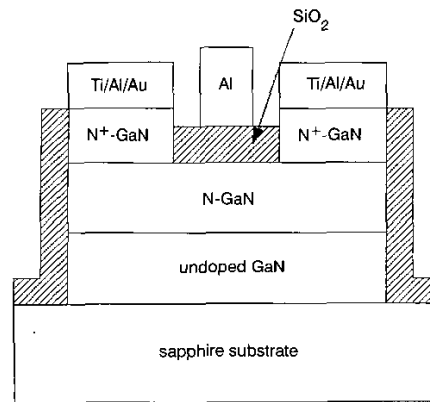


Fig. 1 Schematic structure of n -channel depletion mode GaN MOSFET prepared by MOCVD

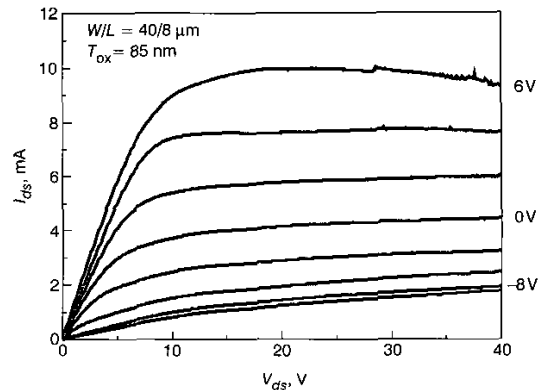


Fig. 2 I_{ds} - V_{ds} characteristics of GaN MOSFET

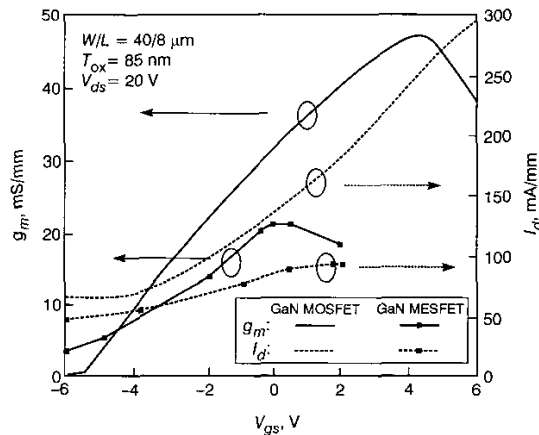


Fig. 3 Transconductance and drain current against gate voltage at $V_{ds} = 20\ \text{V}$

GaN MESFET shown for comparison

Results and discussion: The gate oxide used here is $85\ \text{nm}$ thick with root-mean-square surface roughness of $5.2\ \text{nm}$. The leakage current density at $1\ \text{MV/cm}$ is around $10^{-7}\ \text{A/cm}^2$. The electric field strength for breakdown is larger than $5\ \text{MV/cm}$. The interface state density is about $2 \times 10^{11}\ \text{cm}^{-2}\ \text{eV}^{-1}$. The I-V characteristics of the fabricated GaN MOSFET are shown in Fig. 2 for a device with a gate dimension of $8\ \mu\text{m}$ in channel length and of $40\ \mu\text{m}$ in width. The source-to-drain